



8-2009

Vision-Based, Distributed Control Laws for Motion Coordination of Nonholonomic Robots

Nima Moshtagh

University of Pennsylvania, nima@grasp.upenn.edu

Nathan D. Michael

University of Pennsylvania, nmichael@seas.upenn.edu

Ali Jadbabaie

University of Pennsylvania, jadbabai@seas.upenn.edu

Kostas Daniilidis

University of Pennsylvania, kostas@cis.upenn.edu

Follow this and additional works at: http://repository.upenn.edu/grasp_papers

Recommended Citation

Nima Moshtagh, Nathan D. Michael, Ali Jadbabaie, and Kostas Daniilidis, "Vision-Based, Distributed Control Laws for Motion Coordination of Nonholonomic Robots", . August 2009.

Copyright 2009 IEEE. Reprinted from:

Moshtagh, N.; Michael, N.; Jadbabaie, A.; Daniilidis, K., "Vision-Based, Distributed Control Laws for Motion Coordination of Nonholonomic Robots," Robotics, IEEE Transactions on , vol.25, no.4, pp.851-860, Aug. 2009

URL: <http://ieeexplore.ieee.org/stamp/stamp.jsp?arnumber=5071250&isnumber=5191252>

This material is posted here with permission of the IEEE. Such permission of the IEEE does not in any way imply IEEE endorsement of any of the University of Pennsylvania's products or services. Internal or personal use of this material is permitted. However, permission to reprint/republish this material for advertising or promotional purposes or for creating new collective works for resale or redistribution must be obtained from the IEEE by writing to pubs-permissions@ieee.org. By choosing to view this document, you agree to all provisions of the copyright laws protecting it.

Vision-Based, Distributed Control Laws for Motion Coordination of Nonholonomic Robots

Abstract

In this paper, we study the problem of distributed motion coordination among a group of nonholonomic ground robots. We develop vision-based control laws for parallel and balanced circular formations using a consensus approach. The proposed control laws are distributed in the sense that they require information only from neighboring robots. Furthermore, the control laws are coordinate-free and do not rely on measurement or communication of heading information among neighbors but instead require measurements of bearing, optical flow, and time to collision, all of which can be measured using visual sensors. Collision-avoidance capabilities are added to the team members, and the effectiveness of the control laws are demonstrated on a group of mobile robots.

Keywords

distributed control, mobile robots, motion compensation, multi-robot systems, robot vision, distributed control laws, mobile robots, motion coordination, nonholonomic ground robots, vision-based control laws, Cooperative control, distributed coordination, vision-based control

Comments

Copyright 2009 IEEE. Reprinted from:

Moshtagh, N.; Michael, N.; Jadbabaie, A.; Daniilidis, K., "Vision-Based, Distributed Control Laws for Motion Coordination of Nonholonomic Robots," *Robotics, IEEE Transactions on*, vol.25, no.4, pp.851-860, Aug. 2009

URL: <http://ieeexplore.ieee.org/stamp/stamp.jsp?arnumber=5071250&isnumber=5191252>

This material is posted here with permission of the IEEE. Such permission of the IEEE does not in any way imply IEEE endorsement of any of the University of Pennsylvania's products or services. Internal or personal use of this material is permitted. However, permission to reprint/republish this material for advertising or promotional purposes or for creating new collective works for resale or redistribution must be obtained from the IEEE by writing to pubs-permissions@ieee.org. By choosing to view this document, you agree to all provisions of the copyright laws protecting it.

Vision-Based, Distributed Control Laws for Motion Coordination of Nonholonomic Robots

Nima Moshtagh, *Member, IEEE*, Nathan Michael, *Member, IEEE*, Ali Jadbabaie, *Senior Member, IEEE*,
and Kostas Daniilidis, *Senior Member, IEEE*

Abstract—In this paper, we study the problem of distributed motion coordination among a group of nonholonomic ground robots. We develop vision-based control laws for parallel and balanced circular formations using a consensus approach. The proposed control laws are distributed in the sense that they require information only from neighboring robots. Furthermore, the control laws are coordinate-free and do not rely on measurement or communication of heading information among neighbors but instead require measurements of bearing, optical flow, and time to collision, all of which can be measured using visual sensors. Collision-avoidance capabilities are added to the team members, and the effectiveness of the control laws are demonstrated on a group of mobile robots.

Index Terms—Cooperative control, distributed coordination, vision-based control.

I. INTRODUCTION

COOPERATIVE control of multiple autonomous agents has become a vibrant part of robotics and control theory research. The main underlying theme of this line of research is to analyze and/or synthesize spatially distributed control architectures that can be used for motion coordination of large groups of autonomous vehicles. Some of this research focusses on flocking and formation control [9], [14], [16], [22], [31], and synchronization [2], [39], while others focus on rendezvous, distributed coverage, and deployment [1], [5]. A key assumption implied in all of the previous references is that each vehicle or robot (hereafter called an agent) communicates its position and/or velocity information to its neighbors.

Inspired by the social aggregation phenomena in birds and fish [6], [30], researchers in robotics and control theory have

developed tools, methods, and algorithms for distributed motion coordination of multivehicle systems. Two main collective motions that are observed in nature are *parallel motion* and *circular motion* [21]. One can interpret stabilizing the circular formation as an example of *activity consensus*, i.e., individuals are “moving around” together. Stabilizing the parallel formation is another form of activity consensus in which individuals “move off” together [33]. Circular formations are observed in fish schooling, which is a well-studied topic in ecology and evolutionary biology [6].

In this paper, we present a set of control laws for coordinated motions, such as parallel and circular formations, for a group of planar agents using purely local interactions. The control laws are in terms of *shape variables*, such as the relative distances and relative headings among the agents. However, these parameters are not readily measurable using simple and basic sensing capabilities. This motivates the rewriting of the derived control laws in terms of biologically measurable parameters. Each agent is assumed to have only monocular vision and is also capable of measuring basic visual quantities, such as *bearing angle*, *optical flow* (bearing derivative), and *time to collision*. Rewriting the control inputs in terms of quantities that are locally measurable is equivalent to expressing the inputs in the local body frame. Such a change of coordinate system from a global frame to a local frame provides us with a better intuition on how similar behaviors are carried out in nature.

Verification of the theory through multirobot experiments demonstrated the effectiveness of the vision-based control laws to achieve the desired formations. Of course, in reality, any formation control requires collision avoidance, and indeed, collision avoidance cannot be done without range. In order to improve the experimental results, we provided interagent-collision-avoidance properties to the team members. In this paper, we show that the two tasks of formation keeping and collision avoidance can be done with decoupled additive terms in the control law, where the terms for keeping parallel and circular formations depend only on visual parameters.

This paper is organized as follows. In Section II, we review a number of important related works. Some background information on graph theory and other mathematical tools used in this paper are provided in Section III. The problem statement is given in Section IV. In Sections V and VI, we present the controllers that stabilize a group of mobile agents into parallel and balanced circular formations, respectively. In Section VII, we derive the vision-based controllers that are in terms of the visual measurements of the neighboring agents. In Section VIII, collision-avoidance capabilities are added to the control laws, and their effectiveness is tested on real robots.

Manuscript received February 23, 2008; revised January 31, 2009. First published June 10, 2009; current version published July 31, 2009. This paper was recommended for publication by Associate Editor Z.-W. Luo and Editor J.-P. Laumond upon evaluation of the reviewers' comments. The work of A. Jadbabaie was supported in part by the Army Research Office—Multidisciplinary University Research Initiative (ARO/MURI) under Grant W911NF-05-1-0381, in part by the Office of Naval Research (ONR)/Young Investigator Program 542371, in part by ONR N000140610436, and in part under Contract NSF-ECS-0347285. The work of K. Daniilidis was supported in part under Contract NSF-IIS-0083209, in part under Contract NSF-IIS-0121293, in part under Contract NSF-EIA-0324977, and in part under Contract ARO/MURI DAAD19-02-1-0383.

N. Moshtagh was with the General Robotics, Automation, Sensing, and Perception Laboratory, University of Pennsylvania, Philadelphia, PA 19104 USA. He is now with Scientific Systems Company, Inc., Woburn, MA 01801 USA (e-mail: nmoshtagh@ssci.com).

N. Michael, A. Jadbabaie, and K. Daniilidis are with the General Robotics, Automation, Sensing, and Perception Laboratory, University of Pennsylvania, Philadelphia, PA 19104 USA (e-mail: nmichael@grasp.upenn.edu; jadbabai@grasp.upenn.edu; kostas@grasp.upenn.edu).

Color versions of one or more of the figures in this paper are available online at <http://ieeexplore.ieee.org>.

Digital Object Identifier 10.1109/TRO.2009.2022439

II. RELATED WORK AND CONTRIBUTIONS

The primary contribution of this paper is the presentation of simple control laws to achieve parallel and circular formations that require only visual sensing, i.e., the inputs are in terms of quantities that do not require communication among nearest neighbors. In contrast with the work of Justh and Krishnaprasad [17], Moshtagh and Jadbabaie [27], Paley *et al.* [32], [33], and Sepulchre *et al.* [35], where it is assumed that each agent has access to the values of its neighbors' positions and velocities, we design distributed control laws that use only visual clues from nearest neighbors to achieve motion coordination.

Our approach on deriving the vision-based control laws can be classified as an *image-based visual servoing* [41]. In image-based visual servoing, features are extracted from images, and then the control input is computed as a function of the image features. In [8], [12], and [38], authors use omnidirectional cameras as the only sensor for robots. In [8] and [38], input–output feedback linearization is used to design control laws for leader-following and obstacle avoidance. However, they assume that a specific vertical pose of an omnidirectional camera allows the computation of both bearing and distance. In the work of Prattichizzo *et al.* [12], the distance measurement is not used; however, the leader uses extended Kalman filtering to localize its followers, and computes the control inputs and guides the formation in a *centralized* fashion. In our paper, the control architecture is *distributed*, and we design the formation controllers based on the local interaction among the agents similar to that of [14] and [22]. Furthermore, for our vision-based controllers, no distance measurement is required.

In [25] and [34], circular formations of a multivehicle system under cyclic pursuit is studied. Their proposed strategy is distributed and simple because each agent needs to measure the relative information from only one other agent. It is also shown that the formation equilibria of the multiagent system are generalized polygons. In contrast to [25], our control law is a nonlinear function of the bearing angles, and as a result, our system converges to a different set of stable equilibria.

III. BACKGROUND

In this section, we briefly review a number of important concepts regarding graph theory and regular polygons that we use throughout this paper.

A. Graph Theory

An (undirected) graph \mathcal{G} consists of a vertex set \mathcal{V} and an edge set \mathcal{E} , where an edge is an unordered pair of distinct vertices in \mathcal{G} . If $x, y \in \mathcal{V}$ and $(x, y) \in \mathcal{E}$, then x and y are said to be adjacent, or neighbors, and we denote this by writing $x \sim y$. The number of neighbors of each vertex is its degree. A path of length r from vertex x to vertex y is a sequence of $r + 1$ distinct vertices that start with x and end with y such that consecutive vertices are adjacent. If there is a path between any two vertices of a graph \mathcal{G} , then \mathcal{G} is said to be connected.

The adjacency matrix $A(\mathcal{G}) = [a_{ij}]$ of an (undirected) graph \mathcal{G} is a symmetric matrix with rows and columns indexed by

the vertices of \mathcal{G} , such that $a_{ij} = 1$ if vertex i and vertex j are neighbors, and $a_{ij} = 0$ otherwise. We also assume that $a_{ii} = 0$ for all i . The degree matrix $D(\mathcal{G})$ of a graph \mathcal{G} is a diagonal matrix with rows and columns indexed by \mathcal{V} , in which the (i, i) -entry is the degree of vertex i .

The symmetric singular matrix defined as

$$L(\mathcal{G}) = D(\mathcal{G}) - A(\mathcal{G})$$

is called the Laplacian of \mathcal{G} . The Laplacian matrix captures many topological properties of the graph. The Laplacian L is a positive-semidefinite matrix, and the algebraic multiplicity of its zero eigenvalue (i.e., the dimension of its kernel) is equal to the number of connected components in the graph. The n -dimensional eigenvector associated with the zero eigenvalue is the vector of ones, $\mathbf{1}_n = [1, \dots, 1]^T$. For more information on graph theory, see [13].

B. Regular Polygons

Let $d < n$ be a positive integer, and define $p = n/d$. Let y_1 be a point on the unit circle. Let R_α be clockwise rotation by the angle $\alpha = 2\pi/p$. The *generalized regular polygon* $\{p\}$ is given by the points $y_{i+1} = R_\alpha y_i$ and edges between points i and $i + 1$.

When $d = 1$, the polygon $\{p\}$ is called an ordinary regular polygon, and its edges do not intersect. If $d > 1$ and n and d are coprime, then the edges intersect, and the polygon is a *star*. If n and d have a common factor $l > 1$, then the polygon consists of l traversals of the same polygon with $\{n/l\}$ vertices and edges. If $d = n$, the polygon $\{n/n\}$ corresponds to all points at the same location. If $d = n/2$ (with n even), then the polygon consists of two endpoints and a line between them, with points having an even index on one end and points having an odd index on the other. For more information on regular graphs, see [7].

IV. PROBLEM STATEMENT

Consider a group of n unit-speed planar agents. Each agent is capable of sensing information from its neighbors. The neighborhood set of agent i , that is, \mathcal{N}_i , is the set of agents that can be “seen” by agent i . The precise meaning of “seeing” will be clarified later. The size of the neighborhood depends on the characteristics of the sensors. The neighboring relationship between agents can be conveniently described by a connectivity graph $\mathcal{G} = (\mathcal{V}, \mathcal{E}, \mathcal{W})$.

Definition 1 (Connectivity graph): The connectivity graph $\mathcal{G} = (\mathcal{V}, \mathcal{E}, \mathcal{W})$ is a graph consisting of

- 1) a set of vertices \mathcal{V} indexed by the set of mobile agents;
- 2) a set of edges $\mathcal{E} = \{(i, j) | i, j \in \mathcal{V}, \text{ and } i \sim j\}$;
- 3) a set of positive edge weights for each edge (i, j) .

The neighborhood of agent i is defined by

$$\mathcal{N}_i \doteq \{j | i \sim j\} \subseteq \mathcal{V} \setminus \{i\}.$$

Let \mathbf{r}_i represent the position of agent i , and let \mathbf{v}_i be its velocity vector. The kinematics of each unit-speed agent is

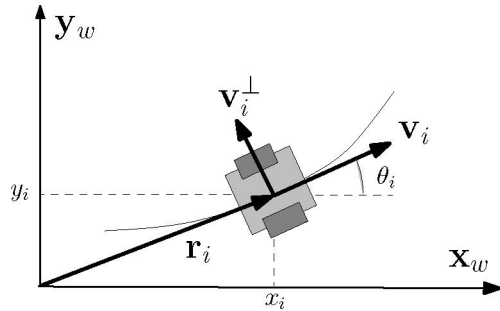


Fig. 1. Trajectory of each agent is represented by a planar Frenet frame.

given by

$$\begin{aligned}\dot{\mathbf{r}}_i &= \mathbf{v}_i \\ \dot{\mathbf{v}}_i &= \omega_i \mathbf{v}_i^\perp \\ \dot{\mathbf{v}}_i^\perp &= -\omega_i \mathbf{v}_i\end{aligned}\quad (1)$$

where \mathbf{v}_i^\perp is the unit vector perpendicular to the velocity vector \mathbf{v}_i (see Fig. 1). The orthogonal pair $\{\mathbf{v}_i, \mathbf{v}_i^\perp\}$ forms a body frame for agent i . We represent the stack vector of all the velocities by $\mathbf{v} = [\mathbf{v}_1^T, \dots, \mathbf{v}_n^T]^T \in \mathbb{R}^{2n \times 1}$.

The control input for each agent is the angular velocity ω_i . Since it is assumed that the agents move with constant unit speed, the force applied to each agent must be perpendicular to its velocity vector, i.e., the force on each agent is a *gyroscopic force*, and it does not change its speed (and hence, its kinetic energy). Thus, ω_i serves as a steering control [16] for each agent.

Let us formally define the formations that we are going to consider.

Definition 2 (Parallel formation): The configuration in which the headings of all agents are the same and velocity vectors are aligned is called the parallel formation.

Note that in this definition, we do not consider the value of the agreed upon velocity but just the fact that the agreement has been reached. At the equilibrium, the relative distances of the agents determine the shape of the formation. Another interesting family of formations is the *balanced circular formation*.

Definition 3 (Balanced circular formation): The configuration where the agents are moving on the same circular trajectory and the geometric center of the agents is fixed is called the balanced circular formation. The shape of such a formation can be represented by an appropriate regular polygon.

In the following sections, we study each formation and design its corresponding distributed control law.

V. PARALLEL FORMATIONS

Our goal in this section is to design a control law for each agent so that the headings of the mobile agents reach an agreement, i.e., their velocity vectors are aligned, thus resulting in a swarm-like pattern. For an arbitrary connectivity graph \mathcal{G} , consider the Laplacian matrix L . We, therefore, define a measure of misalignment as follows [27], [35]:

$$w(\mathbf{v}) = \frac{1}{2} \sum_{i \sim j} |\mathbf{v}_i - \mathbf{v}_j|^2 = \frac{1}{2} \langle \mathbf{v}, \bar{L} \mathbf{v} \rangle \quad (2)$$

where the summation is over all the pairs $(i, j) \in \mathcal{E}$, and $\bar{L} = L \otimes I_2 \in \mathbb{R}^{2n \times 2n}$, with I_2 being the 2×2 identity matrix. The time derivative of $w(\mathbf{v})$ is given by

$$\dot{w}(\mathbf{v}) = \sum_{i=1}^n \langle \dot{\mathbf{v}}_i, (\bar{L} \mathbf{v})_i \rangle = \sum_{i=1}^n \omega_i \langle \mathbf{v}_i^\perp, (\bar{L} \mathbf{v})_i \rangle$$

where $(\bar{L} \mathbf{v})_i \in \mathbb{R}^2$ is the subvector of $\bar{L} \mathbf{v}$ associated with the i th agent. Thus, the following gradient control law guarantees that the potential $w(\mathbf{v})$ decreases monotonically:

$$\omega_i = \kappa \langle \mathbf{v}_i^\perp, (\bar{L} \mathbf{v})_i \rangle = -\kappa \sum_{j \in \mathcal{N}_i} \langle \mathbf{v}_i^\perp, \mathbf{v}_{ij} \rangle \quad (3)$$

where $\kappa < 0$ is the gain, and $\mathbf{v}_{ij} = \mathbf{v}_j - \mathbf{v}_i$.

Remark 1: Let θ_i represent the heading of agent i as measured in a fixed world frame (see Fig. 1). The unit velocity vector \mathbf{v}_i and its orthogonal vector \mathbf{v}_i^\perp are given by $\mathbf{v}_i = [\cos \theta_i \ \sin \theta_i]^T$ and $\mathbf{v}_i^\perp = [-\sin \theta_i \ \cos \theta_i]^T$. Thus, the control input (3) becomes

$$\omega_i = \kappa \sum_{j \in \mathcal{N}_i} \sin(\theta_i - \theta_j), \quad \kappa < 0. \quad (4)$$

It is worth noting that the proposed controller is the one used in the synchronization of the Kuramoto model of coupled nonlinear oscillators, which has been extensively studied in mathematical physics as well as control communities [15], [19], [36]. The same model has also been used for phase regulation of cyclic robotic systems [18].

We have the following theorem [27] that provides a sufficient condition to obtain a parallel formation.

Theorem 1: Consider a system of n unit-speed agents with dynamics (1). If the underlying connectivity graph remains fixed and connected, then by applying control input (4), the system converges to the equilibria of $\boldsymbol{\omega} = [\omega_1 \ \dots \ \omega_n]^T = \mathbf{0}$. Furthermore, the velocity consensus set is locally attractive if $\theta_i \in (-\pi/2, \pi/2)$.

Proof 1: See [27] for the proof. \blacksquare

The *velocity consensus* set is the set of states where all the agents have the same velocity vectors, and it corresponds to the parallel formation, which is defined in Definition 2. Note that $\theta_i \in (-\pi/2, \pi/2) \forall i = \{1, \dots, n\}$ is the sufficient condition that restricts the initial headings to a half-circle. The results can be extended to graphs with switching topology, as shown in [27].

VI. BALANCED CIRCULAR FORMATIONS

The circular formation is a circular relative equilibrium in which all the agents travel around the same circle. We are interested in *balanced circular formations*, which are defined in Definition 3. At the equilibrium, the relative headings and the relative distances of the agents determine the shape of the formation, which can be easily described by a regular polygon.

Let \mathbf{c}_i represent the position of the center of the i th circle with radius $1/\omega_o$, as shown in Fig. 2; thus

$$\mathbf{c}_i = \mathbf{r}_i + \left(\frac{1}{\omega_o} \right) \mathbf{v}_i^\perp.$$

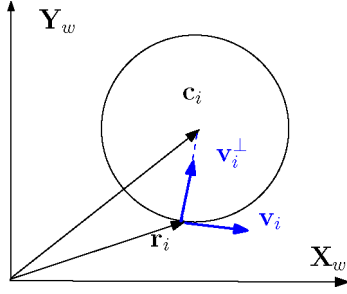


Fig. 2. Center of the circular trajectory is defined as $\mathbf{c}_i = \mathbf{r}_i + (1/\omega_0)\mathbf{v}_i^\perp$.

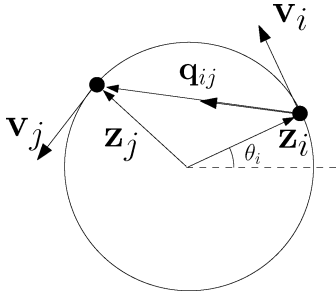


Fig. 3. By a change of coordinate $\mathbf{z}_i = \omega_0(\mathbf{r}_i - \mathbf{c}_i) = -\mathbf{v}_i^\perp$, the problem of generating circular motion in the plane reduces to the problem of balancing the agents on a circle.

The shape controls for driving agents to a circular formation depend on the shape variables $\mathbf{v}_{ij} = \mathbf{v}_j - \mathbf{v}_i$ and $\mathbf{r}_{ij} = \mathbf{r}_j - \mathbf{r}_i$. The relative equilibria of the balanced formation are characterized by $\sum_{i=1}^n \mathbf{v}_i = 0$ and $\mathbf{c}_i = \mathbf{c}_o \in \mathbb{R}^2$ for all $i \in \{1, \dots, n\}$, where \mathbf{c}_o is the fixed geometric center of the agents.

The control input for each agent has two components, which are given by

$$\omega_i = \omega_o + u_i.$$

The constant angular velocity ω_o takes the agents into a circular motion, and u_i sets the agents into a balanced state. In order to design u_i , we express the system in a *rotating frame*, which greatly simplifies the analysis. By the change of variable

$$\mathbf{z}_i = \omega_o(\mathbf{r}_i - \mathbf{c}_i) = -\mathbf{v}_i^\perp$$

the problem reduces to balancing the agents on a unit circle, as shown in Fig. 3. The new coordinate system rotates with angular velocity ω_o . The dynamics in the rotating frame are given by

$$\begin{aligned} \dot{\mathbf{z}}_i &= \mathbf{v}_i u_i \\ \dot{\mathbf{v}}_i &= -\mathbf{z}_i u_i, \quad i = 1, \dots, n. \end{aligned} \quad (5)$$

Unit vector \mathbf{z}_i is normal to the velocity vector. However, in the rotating frame, \mathbf{z}_i represents the position of agent i on the unit circle, which is moving with speed u_i (see Fig. 3).

Let us define $\mathbf{z}_{ij} = \mathbf{z}_j - \mathbf{z}_i$ and $\mathbf{q}_{ij} = \mathbf{z}_{ij}/|\mathbf{z}_{ij}|$ as the unit vector along the new relative position vector \mathbf{z}_{ij} . At the balanced state, the velocity of each agent is perpendicular to $\bar{\mathbf{q}}_i = \sum_{j \in \mathcal{N}_i} \mathbf{q}_{ij}$, which is a vector along the average of the relative position vectors incident to agent i . Thus, the quantity $\langle \mathbf{v}_i, \bar{\mathbf{q}}_i \rangle$ vanishes at the balanced state. Hence, we propose the

following control law for the balanced circular formation:

$$u_i = -\kappa \langle \mathbf{v}_i, \bar{\mathbf{q}}_i \rangle = -\kappa \sum_{j \in \mathcal{N}_i} \langle \mathbf{v}_i, \mathbf{q}_{ij} \rangle, \quad \kappa > 0. \quad (6)$$

The following two theorems [28] present the results when balanced circular formations are attained for a group of unit-speed agents with fixed connectivity graphs. Theorem 2 is for the case when \mathcal{G} is a complete graph, and Theorem 3 is for the ring graph.

Theorem 2: Consider a system of n agents with kinematics (5). Given a complete connectivity graph \mathcal{G} and applying control law (6), the n -agent system (almost) globally asymptotically converges to a balanced circular formation, which is defined in Definition 3.

Proof: See [28] for the proof. ■

The reason for “almost global” stability of the set of balanced states is that there is a measure-zero set of states where the equilibrium is unstable. This set is characterized by those configurations that m agents are at antipodal position from the other $n - m$ agents, where $1 \leq m < n/2$. Next, we consider the situation that the connectivity graph has a ring topology $\mathcal{G}^{\text{ring}}$.

Theorem 3: Consider a system of n agents with kinematics (5). Suppose the connectivity graph has the ring topology $\mathcal{G}^{\text{ring}}$ and that each agent applies the balancing control law (6). Then, the relative headings will converge to the same angle ϕ_o . If $\phi_o \in (\pi/2, 3\pi/2)$, the balanced state is locally exponentially stable.

Proof: See [28] for the proof. ■

At the equilibrium, the final configuration for $\mathcal{G}^{\text{ring}}$ is a regular polygon $\{n/d\}$ in which the relative angle between two connected nodes is $\phi_o = 2\pi d/n$. From Theorem 3, if this angle satisfies $\phi_o \in (\pi/2, 3\pi/2)$, then the balanced state is stable. Thus, the stable configuration corresponds to a polygon with $d \in (n/4, 3n/4)$.

For example, for $n = 5$, the stable formations are polygons $\{5/3\}$ and $\{5/4\}$, which are the same polygons as obtained with reverse ordering of the nodes. For $n = 4$, the stable formation is $\{4/2\}$. Actually, simulations suggest that the largest region of attraction for n even belongs to a polygon $\{n/d\}$, with $d = n/2$, and for n odd, it is a *star* polygon $\{n/d\}$, with $d = (n \pm 1)/2$.

VII. VISION-BASED CONTROL LAWS

Note that the control inputs (4) and (6) for parallel and circular formations depend on the *shape variables*, i.e., relative headings and positions, which are not directly measurable using visual sensors, such as a single camera on a robot, because estimation of the relative position and motion requires binocular vision. This motivates us to rewrite inputs (4) and (6) in terms of parameters that are entirely measurable using a simple visual sensor. Next, we define the visual parameters that we will use to derive the vision-based control laws.

Bearing angle—Let $\mathbf{r}_i = [x_i \ y_i]^T$ be the location of agent i in a fixed world frame, and let $\mathbf{v}_i = [\dot{x}_i \ \dot{y}_i]^T$ be its velocity vector. The heading or orientation of agent i is then given by

$$\theta_i = \text{atan2}(\dot{y}_i, \dot{x}_i). \quad (7)$$

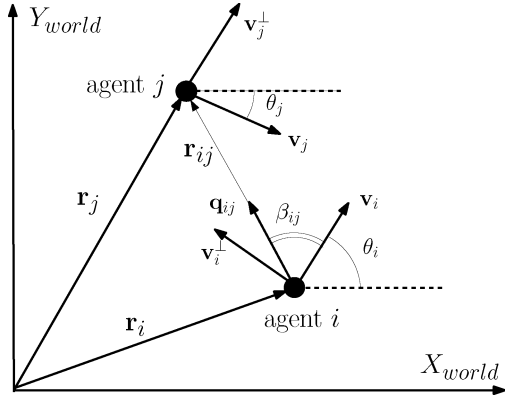


Fig. 4. Bearing angle β_{ij} is measured as the angle between the velocity vector (along body x -axis) and vector \mathbf{r}_{ij} , which connects the two neighboring agents.

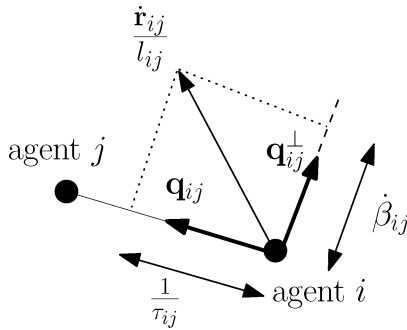


Fig. 5. Optical flow $\dot{\beta}_{ij}$ and loom $1/\tau_{ij}$ can be written in terms of the scaled relative velocity.

As per the earlier definitions and knowing that agents have unit speed, dynamic model (1) becomes the unicycle model:

$$\begin{aligned}\dot{x}_i &= \cos \theta_i \\ \dot{y}_i &= \sin \theta_i \\ \dot{\theta}_i &= \omega_i\end{aligned}\quad (8)$$

where ω_i is the angular velocity of agent i . The bearing angle β_{ij} , which is defined as the relative angle between $\mathbf{q}_{ij} = \mathbf{r}_{ij}/|\mathbf{r}_{ij}|$ and \mathbf{v}_i , is given by (see Fig. 4)

$$\beta_{ij} \doteq \text{atan2}(y_i - y_j, x_i - x_j) - \theta_i. \quad (9)$$

Optical flow is the rate of change of the bearing β_{ij} , which corresponds to the relative motion of agents i and j , as seen by agent i . One can see from Fig. 5 that $\dot{\beta}_{ij}$ is equal to the projection of the scaled relative velocity vector $\dot{\mathbf{r}}_{ij}/l_{ij}$, which is perpendicular to the unit bearing vector $\mathbf{q}_{ij} = [\cos \beta_{ij} \sin \beta_{ij}]^T$. More precisely

$$\dot{\beta}_{ij} = \left\langle \frac{\dot{\mathbf{r}}_{ij}}{l_{ij}}, \mathbf{q}_{ij}^\perp \right\rangle \quad (10)$$

where $l_{ij} = |\mathbf{r}_{ij}|$. Note that only one optical flow measurement per agent is taken, thus making it impossible to rely on structure from motion algorithms. Regarding optical flow, see [3].

Time to collision τ_{ij} can be estimated from the ratio of area change to area or from the divergence of the optical flow [4].

Incidentally, experimental evidence suggests that several animal species, including pigeons and flies, are capable of estimating time to collision [10], [20], [40], or the inverse of time to collision, known as *loom* [23]. Actually “loom” is the parameter that we need, which is given by

$$\frac{1}{\tau_{ij}} = \frac{\dot{a}_{ij}}{a_{ij}} = \frac{\dot{l}_{ij}}{l_{ij}} = \left\langle \frac{\dot{\mathbf{r}}_{ij}}{l_{ij}}, \mathbf{q}_{ij} \right\rangle \quad (11)$$

where the last equality can be deduced from Fig. 5. Note that the measurement of time to collision τ_{ij} (or loom) is not equivalent to the measurement of the relative distance between the agents as is usually the case in visual motion problems. This is due to the fact that time to collision can only recover the distance up to an unknown factor, which, in our case, is different for every neighboring agent.

Thus, to formally define sensing, we assume that each agent i can measure

- 1) β_{ij} as the bearing angle;
- 2) $\dot{\beta}_{ij}$ as the optical flow;
- 3) τ_{ij} as time to collision;

for any agent j in the set of neighbors \mathcal{N}_i . In the following, we show how to write the control inputs (4) and (6) in terms of the measurable quantities defined before.

A. Parallel Formation

In this section, we derive a vision-based control law for generating parallel formations within a group of nonholonomic agents that does not require the direct communication of the heading information [unlike input (4)]. In order to derive such a vision-based control law, we normalized each term in (4) by the relative distance l_{ij} , because the *normalized* relative velocity vector can be written in terms of the measurable quantities of optical flow and time to collision, as shown in Fig. 5. Consider the following modified version of the control law (4) with $\kappa < 0$:

$$\omega_i = \sum_{j \in \mathcal{N}_i} \frac{-\kappa}{|\mathbf{r}_{ij}|} \langle \mathbf{v}_i^\perp, \mathbf{v}_{ij} \rangle = \sum_{j \in \mathcal{N}_i} \frac{\kappa}{l_{ij}} \sin(\theta_i - \theta_j). \quad (12)$$

Now, we derive the vision-based control law for the parallel formation that is equivalent to (12). The equation that describes the relative motion of agents i and j is given by

$$\dot{\mathbf{r}}_{ij} = -\omega_i \times \mathbf{r}_{ij} + \mathbf{v}_{ij} \quad (13)$$

where ω_i is the body angular velocity vector of agent i , and all vectors in this equation are expressed in the body frame of agent i . We normalize the optical flow equation (13) by dividing it by l_{ij} to get

$$\frac{\dot{\mathbf{r}}_{ij}}{l_{ij}} = -\omega_i \times \mathbf{q}_{ij} + \frac{\mathbf{v}_{ij}}{l_{ij}} \quad \forall j \in \mathcal{N}_i. \quad (14)$$

Equation (14) holds for all the agents that are in \mathcal{N}_i . Thus, we sum (14) over all $j \in \mathcal{N}_i$ to get

$$\sum_{j \in \mathcal{N}_i} \frac{\dot{\mathbf{r}}_{ij}}{l_{ij}} = -\sum_{j \in \mathcal{N}_i} \omega_i \times \mathbf{q}_{ij} + \sum_{j \in \mathcal{N}_i} \frac{\mathbf{v}_{ij}}{l_{ij}}. \quad (15)$$

Note that all the parameters in (15) are expressed in the body frame of agent i . The goal is to solve (15) for input ω_i so that it is only a function of the measurable quantities defined earlier.

Let us use the following notation:

$$\mathbf{m}_i = \sum_{j \in \mathcal{N}_i} \frac{\dot{\mathbf{r}}_{ij}}{l_{ij}}, \quad \mathbf{q}_i = \sum_{j \in \mathcal{N}_i} \mathbf{q}_{ij}.$$

It is easy to show that \mathbf{m}_i is a measurable vector. To see this, we differentiate $\mathbf{r}_{ij} = l_{ij} \mathbf{q}_{ij}$, and we get $\dot{\mathbf{r}}_{ij} = \dot{l}_{ij} \mathbf{q}_{ij} + l_{ij} \dot{\mathbf{q}}_{ij}$. Therefore,

$$\mathbf{m}_i = \sum_{j \in \mathcal{N}_i} \frac{\dot{\mathbf{r}}_{ij}}{l_{ij}} = \sum_{j \in \mathcal{N}_i} \left(\frac{\mathbf{q}_{ij}}{\tau_{ij}} + \dot{\mathbf{q}}_{ij} \right). \quad (16)$$

The bearing vector \mathbf{q}_{ij} and the optical flow vector $\dot{\mathbf{q}}_{ij}$ in the body frame of agent i are given by

$$\mathbf{q}_{ij} = \begin{bmatrix} \cos \beta_{ij} \\ \sin \beta_{ij} \end{bmatrix}, \quad \dot{\mathbf{q}}_{ij} = \dot{\beta}_{ij} \begin{bmatrix} -\sin \beta_{ij} \\ \cos \beta_{ij} \end{bmatrix} = \dot{\beta}_{ij} \mathbf{q}_{ij}^\perp.$$

Therefore, \mathbf{m}_i is measurable (see Fig. 5).

Given that the velocity of agent i is along the x -axis of its body frame, then vectors \mathbf{v}_i and \mathbf{v}_j can be expressed in the i th body frame as

$$\mathbf{v}_i = \begin{bmatrix} 1 \\ 0 \end{bmatrix}, \quad \mathbf{v}_j = \begin{bmatrix} \cos(\theta_j - \theta_i) \\ \sin(\theta_j - \theta_i) \end{bmatrix} = \begin{bmatrix} \cos(\theta_i - \theta_j) \\ -\sin(\theta_i - \theta_j) \end{bmatrix}.$$

By substituting for ω_i and \mathbf{v}_{ij} in (15), we get

$$\mathbf{m}_i = - \begin{bmatrix} 0 & -\omega_i \\ \omega_i & 0 \end{bmatrix} \mathbf{q}_i + \sum_{j \in \mathcal{N}_i} \frac{1}{l_{ij}} \begin{bmatrix} \cos(\theta_i - \theta_j) - 1 \\ -\sin(\theta_i - \theta_j) \end{bmatrix}.$$

This relation gives us two sets of linear equations. The second equation is

$$(\mathbf{m}_i)_y = -\omega_i (\mathbf{q}_i)_x - \sum_{j \in \mathcal{N}_i} \frac{1}{l_{ij}} \sin(\theta_i - \theta_j) \quad (17)$$

where $(\cdot)_x$ and $(\cdot)_y$ are the x and y components of a vector. We can see that the last term on the right-hand side is actually the input given by (12) that is scaled by factor $1/\kappa$. Hence, (17) becomes

$$(\mathbf{m}_i)_y = -\omega_i (\mathbf{q}_i)_x + \frac{1}{\kappa} \omega_i$$

which can be solved for ω_i . After substituting for $(\mathbf{m}_i)_y$ and $(\mathbf{q}_i)_x$, we get

$$\omega_i = \frac{-\kappa \sum_{j \in \mathcal{N}_i} \left((1/\tau_{ij}) \sin \beta_{ij} + \dot{\beta}_{ij} \cos \beta_{ij} \right)}{1 + \kappa \sum_{j \in \mathcal{N}_i} \cos \beta_{ij}}, \quad \kappa < 0. \quad (18)$$

This is the vision-based control law that is equivalent to (4) and takes a group of kinematic agents to a parallel formation. See Section VIII for the experimental verification of the results.

B. Balanced Circular Formation

As we will see shortly, the only visual parameter that is required to generate a balanced circular formation is the *bearing angle* β_{ij} . It is remarkable that we can generate interesting global patterns using only a single measurement of the bearing angle.

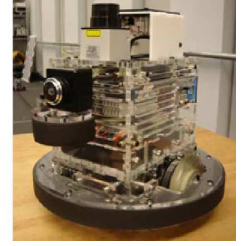
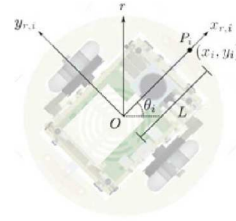


Fig. 6. Scarab is a small robot with a differential drive axle. LED markers are placed on top of each Scarab for pose estimation.

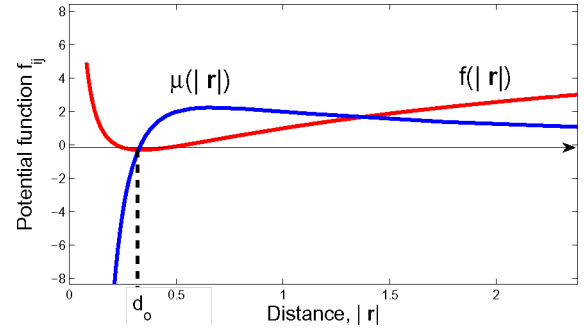


Fig. 7. Artificial potential function $f_{ij} = (d_0/|r_{ij}|) + \log |r_{ij}|$, where d_0 is the desired distance between the neighboring agents. The variable μ_{ij} is the norm of its gradient.

Note that the inner product of two vectors is independent of the coordinate system in which they are expressed. Thus, given $\mathbf{v}_i = [10]^T$ and $\mathbf{q}_{ij} = [\cos \beta_{ij} \sin \beta_{ij}]^T$ in the body frame of agent i , the control input for balanced circular formation can be written as ($\kappa > 0$)

$$\omega_i = \omega_o - \kappa \sum_{j \in \mathcal{N}_i} \langle \mathbf{v}_i, \mathbf{q}_{ij} \rangle = \omega_o - \kappa \sum_{j \in \mathcal{N}_i} \cos \beta_{ij}. \quad (19)$$

Input (19) is the desired vision-based control input that drives a group of nonholonomic planar agents into a balanced circular formation.

VIII. EXPERIMENTS

In this section, we show the results of experimental tests for balanced circular and parallel formations, but first, let us describe the experimental test bed.

Robots: We use a series of small form-factor robots called Scarab [26]. The Scarab is a $20 \times 13.5 \times 22.2$ cm³ indoor ground platform, with a mass of 8 kg. Each Scarab is equipped with a differential drive axle placed at the center of the length of the robot with a 21-cm wheel base (see Fig. 6). Each Scarab is equipped with an onboard computer, a power-management system, and wireless communication. Each robot is actuated by stepper motors, which allows us to model it as a point robot with unicycle kinematics (8) for its velocity range. The linear velocity of each robot is bounded at 0.2 m/s. Each robot is able to rotate about its center of mass at speeds below 1.5 rad/s. Typical angular velocities resulting from the control law were below 0.5 rad/s.

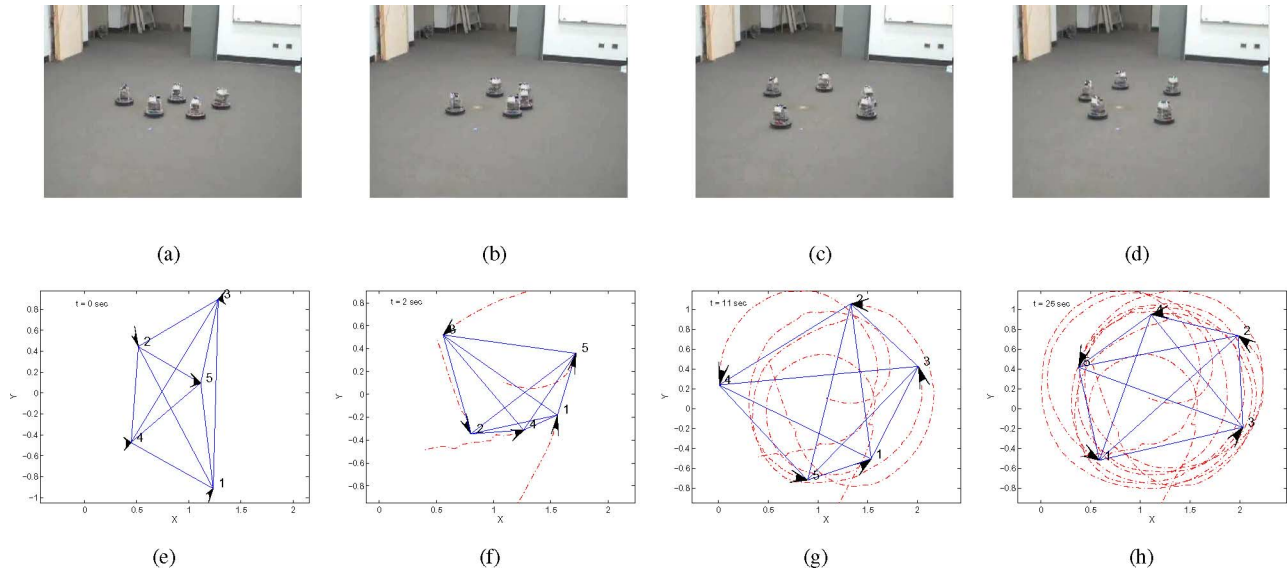


Fig. 8. Five *Scarabs* form a circular formation starting with a complete-graph topology. (a) At time $t = 0$, robots start at random positions and orientations. (b) $t = 2$ s. (c) $t = 11$ s. (d) At $t = 25$ s, the robots reach a stable balanced configuration around a circle with radius of 1 m. (e)–(h) Actual trajectories of the robots and their connectivity graph at the times specified before. (h) Final configuration is a regular polygon.

Software: Every robot is running identical modularized software with well-defined interfaces connecting modules via the *Player* robot architecture system [11], which consists of libraries that provide access to communication and interface functionality. The *Player* also provides a close collaboration with the 3-D physics-based simulation environment *Gazebo*, which provides the powerful ability to transition transparently from code running on simulated hardware to real hardware.

Infrastructure: In the experiments, visibility of the robot's set of neighbors is the main issue. Using omnidirectional cameras seems to be a natural solution. However, using onboard sensors would make the implementation quite challenging. Since the focus of this paper was not the vision or estimation problem, we have chosen to use an overhead tracking system to solve the occlusion problem and obtain more accurate bearing and time-to-collision information.

The tracking system consists of LED markers on the robots and eight overhead cameras. This ground-truth-verification system can locate and track the robots with position error of approximately 2 cm and an orientation error of 5° . The overhead tracking system allows control algorithms to assume that pose is known in a global reference frame. The process and measurement models fuse local odometry information and tracking information from the camera system.

Each robot locally estimates its pose based on the globally available tracking system data and local motion, using an extended Kalman filter. We process global overhead tracking information but hide the global state of the system from each robot, thus providing only the current state of the robot and the positions of each robot's set of neighbors. In this way, we use the tracking system in lieu of an interrobot sensor implementation.

In all the experiments, the neighborhood relations, i.e., the connectivity graphs, are fixed and undirected. Each robot computes the visual measurements with respect to its neighbors

from (9) and (11). The conclusions for each set of experiments are drawn from significant number of successful trials that supported the effectiveness of the designed controllers. The results of the experiments are provided in the following sections.

A. Implementation With Collision Avoidance

In reality, any formation control requires collision avoidance, and indeed, collision avoidance cannot be done without range. Here, we show that the two tasks can be done with decoupled additive terms in the control law, where the terms for parallel and circular formations depend only on visual information.

An interagent potential function [29], [37] is defined to ensure collision avoidance and cohesion of the formation during the experiments. The control law from this artificial potential function results in simple steering behaviors known as *separation* and *cohesion*. The potential function $f_{ij}(|\mathbf{r}_{ij}|)$ is a symmetric function of the distance $|\mathbf{r}_{ij}|$ between agents i and j and is defined as follows [37].

Definition 4 (Potential function): Potential f_{ij} is a differentiable, nonnegative function of the distance $|\mathbf{r}_{ij}|$ between agents i and j such that the following hold.

- 1) $f_{ij} \rightarrow \infty$ as $|\mathbf{r}_{ij}| \rightarrow 0$.
- 2) f_{ij} attains its unique minimum when agents i and j are located at a desired distance.

The requirements for f_{ij} , which are given in Definition 4, support a large class of functions. A common potential function is shown in Fig. 7. The total potential function of agent i is then given by

$$f_i = \sum_{j \in \mathcal{N}_i} f_{ij}(|\mathbf{r}_{ij}|). \quad (20)$$

The collision-avoidance term in the control input must insert a gyroscopic force that is perpendicular to the velocity vector

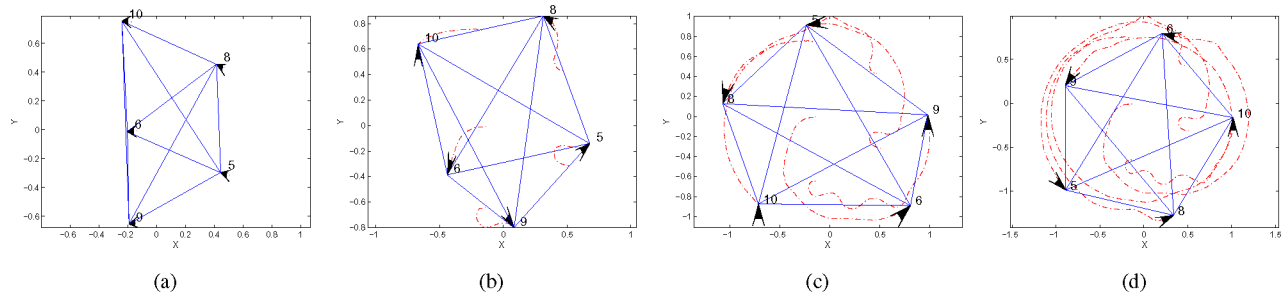


Fig. 9. Five *Scarabs* form a circular formation starting with a complete-graph topology while avoiding collisions. (a) $t = 0$ s. (b) $t = 8$ s. (c) $t = 20$ s. (d) At $t = 36$ s, the robots reach a stable balanced configuration around a circle with radius of 1 m. (a)–(d) Actual trajectories of the robots and their connectivity graph at the times specified before.

\mathbf{v}_i (along \mathbf{v}_i^\perp), and it must also be proportional to the negative gradient of the total potential function f_i of agent i . Thus, as a result, the collision-avoidance controller takes the form

$$\alpha_i = -\kappa_p \langle \mathbf{v}_i^\perp, \nabla_{\mathbf{r}_i} f_i \rangle, \quad \kappa_p > 0. \quad (21)$$

The total control inputs for parallel and balanced circular formations include the additional component α_i :

$$\omega_i = \omega_i^{\text{formation}} + \alpha_i \quad (22)$$

where $\omega_i^{\text{formation}}$ is the vision-based control input given by (18) for parallel formation or (19) for the circular formation, and α_i steers the agents to avoid collisions or pull them together if they are too far apart.

B. Balanced Circular Formations

The result of the experiments for the complete-graph topology and the ring topology are summarized in the following sections.

1) *Complete-Graph Topology*: First, we applied the bearing-only control law (19) to a group of $n = 5$ robots without considering collision avoidance among the agents. In Fig. 8(a) through (d), snapshots from the actual experiment are shown, and in Fig. 8(e) through (h), the corresponding trajectories, which are generated from overhead tracking information, are demonstrated. Note that for the complete-graph topology, the ordering of the robots in the final configuration is not unique; it depends on the initial positions.

Since no collision avoidance was implemented in the experiments of Fig. 8, the robots could become undesirably close to one another, as can be seen in Fig. 8(b). However, by applying control input (22), it can be seen that no collisions occur among the robots as they reach the equilibrium. The actual trajectories of $n = 5$ robots for this scenario are shown in Fig. 9. The comparison of the potential energies of the system with and without α_i term [see (21)] are presented in Fig. 10. The potential energy of the system is computed from $f = \sum_{i=1}^n f_i$, where f_i is given by (20). The peak in Fig. 10(a) corresponds to the configuration observed in Fig. 8(b), where robots become too close to each other. By using the control input (22), the potential energy of the five-agent system monotonically decreases [see Fig. 10(b)], and the system stabilizes to a state where the potential energy of the entire system is minimized.

2) *Ring Topology*: If each robot can “sense” only two other robots in the group, the topology of the connectivity graph will

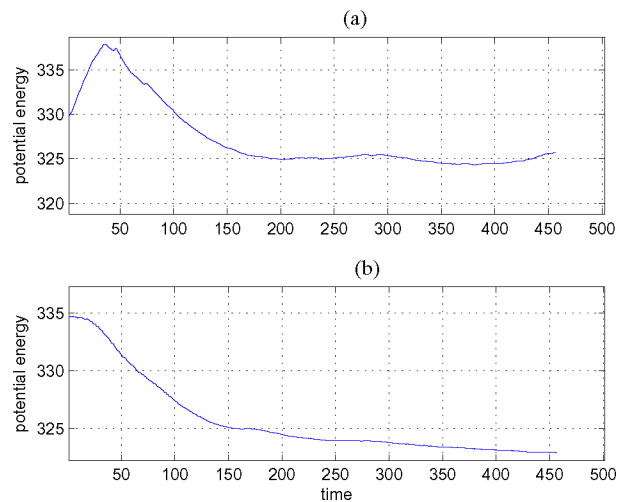


Fig. 10. Comparison of the values of the five-agent system’s potential energy while robots are applying (a) control input (19) and (b) control input (22) with collision avoidance.

be a ring topology. Since the connectivity graph is assumed fixed, the agents need to be numbered during the experiments.

For n even, the balancing term in the control input drives the agents into a balanced circular formation, which is given by polygon $\{n/d\}$, with $d = n/2$. This requires that robots with even indices stay on one side of a line segment and robots with odd indices stay at the other side (not physically possible). However, the collision-avoidance term keeps the agents at the desired separation.

For n odd, the largest region of attraction of the balancing input is the star polygon $\{n/d\}$, with $d = (n \pm 1)/2$; therefore, only two orderings of the robots are possible in the final circular formation. Fig. 11 shows that in our experiment, the robots are stabilized to the star polygon $\{5/3\}$.

Remark 2: When the communication graph is a fixed, directed graph with a ring topology, where agent i could see only agent $(i + 1)/\text{mod}(n)$, then the n -agent system would behave like a team of robots in cyclic pursuit [25].

C. Parallel Formation With Fixed Topology

The space limitations imposed by the ground-truth-verification system prohibited us from testing the vision-based

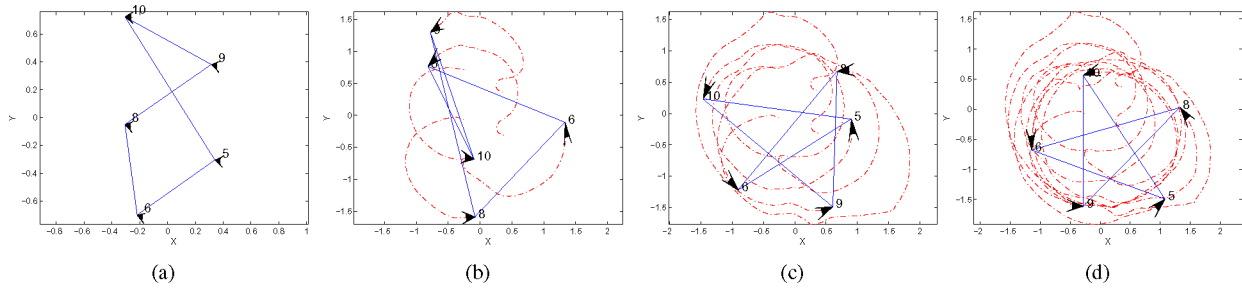


Fig. 11. Five *Scarabs* form a circular formation starting with a ring topology while avoiding collisions. (a) $t = 0$ s. (b) $t = 16$ s. (c) $t = 40$ s. (d) At $t = 80$ s, the robots reach a stable balanced configuration, which is the star polygon $\{5/3\}$ around a circle with radius of 1 m. (a)–(d) Actual trajectories of the robots and their connectivity graph at the times specified before.

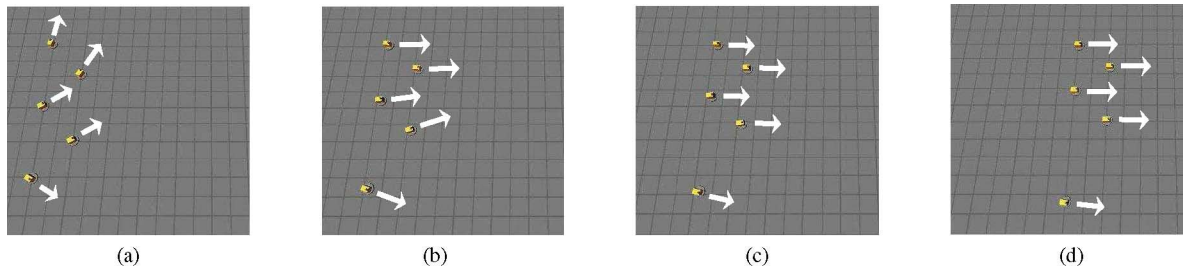


Fig. 12. Five *Scarabs*, starting with different initial orientations, apply the vision-based control input (18) to achieve a parallel formation. The simulation is done in the simulator *Gazebo*. (a) $t = 0$ s. (b) $t = 1$ s. (c) $t = 3$ s. (d) $t = 7$ s.

control law for parallel motion directly on *Scarabs*. However, simulations were made in *Gazebo*, which is a physics-based simulator. *Gazebo* simulations accurately reflect the robot dynamics and sensing capabilities, while permitting evaluation of the same code used during hardware experimentation. Fig. 12 shows snapshots of the *Gazebo* simulation for a group of five *Scarabs*, with each applying (22): the vision-based control input plus the collision-avoidance input.

IX. CONCLUSION AND FUTURE WORK

The central contribution of this paper is to provide simple vision-based control laws to achieve parallel and balanced circular formations. Of course, in reality, any formation control requires collision avoidance, and indeed, collision avoidance cannot be done without range. We have shown here that the two tasks can be done with decoupled additive terms in the control law, where the term for formation control depends only on visual information.

The vision-based control laws were functions of quantities such as bearing, optical flow, and time to collision, all of which could be measured from images. Only bearing measurements were needed for achieving a balanced circular formation, whereas for a parallel formation, additional measurements of optical flow and time to collision were required. We verified the effectiveness of the theory through multirobot experiments.

Note that when we work with robots that have limited field of view, directed connectivity graphs [24] come into play. The study of motion coordination in the presence of directed communication graphs is the subject of ongoing work.

REFERENCES

- [1] M. Batalin, G. S. Sukhatme, and M. Hattig, "Mobile robot navigation using a sensor network," in *Proc. IEEE Int. Conf. Robot. Autom.*, 2004, pp. 636–642.
- [2] R. W. Beard and V. Stepanyan, "Synchronization of information in distributed multiple vehicle coordinated control," in *Proc. IEEE Conf. Decis. Control*, 2003, pp. 2029–2034.
- [3] S. S. Beauchemin and J. L. Barron, "The computation of optical flow," *ACM Comput. Surv.*, vol. 27, pp. 433–467, 1995.
- [4] R. Cipolla and A. Blake, "Surface orientation and time to contact from image divergence and deformation," in *Proc. 2nd Eur. Conf. Comput. Vis.*, 1992, pp. 187–202.
- [5] J. Cortes, S. Martinez, T. Karatas, and F. Bullo, "Coverage control for mobile sensing networks," *IEEE Trans. Robot. Autom.*, vol. 20, no. 2, pp. 243–255, Feb. 2004.
- [6] I. D. Couzin, J. Krause, R. James, G. D. Ruxton, and N. R. Franks, "Collective memory and spatial sorting in animal groups," *J. Theor. Biol.*, vol. 218, no. 1, pp. 1–11, 2002.
- [7] H. S. M. Coxeter, *Regular Polytopes*. Chelmsford, MA: Courier Dover, 1973.
- [8] A. Das, R. Fierro, V. Kumar, J. Ostrowski, J. Spletzer, and C. J. Taylor, "Vision based formation control of multiple robots," *IEEE Trans. Robot. Autom.*, vol. 18, no. 5, pp. 813–825, Oct. 2002.
- [9] W. Dong and J. A. Farrell, "Cooperative control of multiple nonholonomic mobile agents," *IEEE Trans. Autom. Control*, vol. 53, no. 6, pp. 1434–1448, Jul. 2008.
- [10] S. N. Fry, R. Sayaman, and M. H. Dickinson, "The aerodynamics of free-flight maneuvers in *Drosophila*," *Science*, vol. 300, pp. 495–498, 2003.
- [11] B. Gerkey, R. T. Vaughan, and A. Howard, "The player/stage project: Tools for multi-robot and distributed sensor systems," in *Proc. Int. Conf. Adv. Robot.*, Jun. 2003, pp. 317–323.
- [12] D. Prattichizzo, G. L. Mariottini, G. J. Pappas, and K. Daniilidis, "Vision-based localization of leader-follower formations," in *Proc. 44th IEEE Conf. Decis. Control*, Dec. 2005, pp. 635–640.
- [13] C. Godsil and G. Royle, *Algebraic Graph Theory*. (Graduate Texts in Mathematics 207). New York: Springer-Verlag, 2001.
- [14] A. Jadbabaie, J. Lin, and A. S. Morse, "Coordination of groups of mobile autonomous agents using nearest neighbor rules," *IEEE Trans. Autom. Control*, vol. 48, no. 6, pp. 988–1001, Jun. 2003.
- [15] A. Jadbabaie, N. Motee, and M. Barahona, "On the stability of Kuramoto model of coupled nonlinear oscillators," in *Proc. Amer. Control Conf.*, Jul. 2004, vol. 5, pp. 4296–4301.

- [16] E. W. Justh and P. S. Krishnaprasad, "Simple control laws for UAV formation flying," Naval Res. Lab., Washington, DC, Tech. Rep., Jun. 2002.
- [17] E. W. Justh and P. S. Krishnaprasad, "Equilibria and steering laws for planar formations," *Syst. Control Lett.*, vol. 52, no. 1, pp. 25–38, May 2004.
- [18] E. Klavins and D. E. Koditschek, "Phase regulation of decentralized cyclic robotic systems," *Int. J. Robot. Autom.*, vol. 21, no. 3, pp. 257–275, 2002.
- [19] Y. Kuramoto, *Cooperative Dynamics in Complex Physical Systems*. Berlin, Germany: Springer-Verlag, 1989.
- [20] D. N. Lee and P. E. Reddish, "Plummeting gannets—A paradigm of ecological optics," *Nature*, vol. 5830, pp. 293–294, 1981.
- [21] H. Levine, E. Ben-Jacob, I. Cohen, and W.-J. Rappel, "Swarming patterns in microorganisms: Some new modeling results," in *Proc. IEEE Conf. Decis. Control*, Dec. 2006, pp. 5073–5077.
- [22] Z. Lin, M. Broucke, and B. Francis, "Local control strategies for groups of mobile autonomous agents," *IEEE Trans. Autom. Control*, vol. 49, no. 4, pp. 622–629, Apr. 2004.
- [23] W. MacFarland and S. Levin, "Modeling the effects of current on prey acquisition in planktivorous fishes," *Mar. Fresh. Behav. Physiol.*, vol. 35, no. 1/2, pp. 69–85, 2002.
- [24] J. A. Marshall and M. E. Broucke, "On invariance of cyclic group symmetries in multiagent formations," in *Proc. 44th IEEE Conf. Decis. Control, Eur. Control Conf.*, Seville, Spain, Dec. 2005, pp. 746–751.
- [25] J. A. Marshall, M. E. Broucke, and B. A. Francis, "Formations of vehicles in cyclic pursuit," *IEEE Trans. Autom. Control*, vol. 49, no. 11, pp. 1963–1974, Nov. 2004.
- [26] N. Michael, J. Fink, and V. Kumar, "Controlling a team of ground robots via an aerial robot," in *Proc. IEEE/RSJ Int. Conf. Intell. Robots Syst.*, San Diego, CA, Nov. 2007, pp. 965–970.
- [27] N. Moshagh and A. Jadbabaie, "Distributed geodesic control laws for flocking of nonholonomic agents," *IEEE Trans. Autom. Control*, vol. 52, no. 4, pp. 681–686, Apr. 2007.
- [28] N. Moshagh, N. Michael, A. Jadbabaie, and K. Daniilidis, "Distributed, bearing-only control laws for circular formations of ground robots," presented at the Robot.: Sci. Syst. Conf., Zurich, Switzerland, Jun. 2008.
- [29] P. Ogren, E. Fiorelli, and N. E. Leonard, "Cooperative control of mobile sensing networks: Adaptive gradient climbing in a distributed environment," *IEEE Trans. Autom. Control*, vol. 49, no. 8, pp. 1292–1302, Aug. 2004.
- [30] A. Okubo, "Dynamical aspects of animal grouping: Swarms, schools, flocks, and herds," *Adv. Biophys.*, vol. 22, pp. 1–94, 1986.
- [31] R. Olfati-Saber, "Flocking for multiagent dynamical systems: Algorithms and theory," *IEEE Trans. Autom. Control*, vol. 51, no. 3, pp. 401–420, Mar. 2006.
- [32] D. Paley, N. Leonard, and R. Sepulchre, "Oscillator models and collective motion: Splay state stabilization of self-propelled particles," in *Proc. 44th IEEE Conf. Decis. Control, Eur. Control Conf.*, Seville, Spain, Dec. 2005, pp. 3935–3940.
- [33] D. A. Paley, N. E. Leonard, R. Sepulchre, D. Grunbaum, and J. K. Parrish, "Oscillator models and collective motion," *IEEE Control Syst. Mag.*, vol. 27, no. 4, pp. 89–105, Aug. 2007.
- [34] M. Pavone and E. Frazzoli, "Decentralized policies for geometric pattern formation and path coverage," *ASME J. Dyn. Syst., Meas., Control*, vol. 129, pp. 633–643, 2007.
- [35] R. Sepulchre, D. Paley, and N. Leonard, "Stabilization of planar collective motion: All-to-all communication," *IEEE Trans. Autom. Control*, vol. 52, no. 5, pp. 811–824, May 2007.
- [36] S. H. Strogatz, "From Kuramoto to Crawford: Exploring the onset of synchronization in populations of coupled nonlinear oscillators," *Phys. D*, vol. 143, pp. 1–20, 2000.
- [37] H. Tanner, A. Jadbabaie, and G. Pappas, "Flocking in fixed and switching networks," *IEEE Trans. Autom. Control*, vol. 52, no. 5, pp. 863–868, May 2007.
- [38] R. Vidal, O. Shakernia, and S. Sastry, "Formation control of nonholonomic mobile robots with omnidirectional visual servoing and motion segmentation," in *Proc. IEEE Int. Conf. Robot. Autom.*, Sep. 2003, vol. 1, pp. 584–589.
- [39] W. Wang and J. J. E. Slotine, "On partial contraction analysis for coupled nonlinear oscillators," Nonlinear Syst. Lab. Mass. Inst. Technol., Cambridge, MA, Tech. Rep., 2003.
- [40] Y. Wang and B. J. Frost, "Time to collision is signalled by neurons in the nucleus rotundus of pigeons," *Nature*, vol. 356, no. 6366, pp. 236–238, 1992.
- [41] H. Zhang and J. P. Ostrowski, "Visual motion planning for mobile robots," *IEEE Trans. Robot. Autom.*, vol. 18, no. 2, pp. 199–208, Apr. 2002.



Nima Moshagh (S'04–M'09) received the B.S. degree from Pennsylvania State University, University Park, in 2003 and the Ph.D. degree in electrical engineering from the University of Pennsylvania, Philadelphia, in 2008.

He is currently a Research Scientist at the GRASP Laboratory, University of Pennsylvania. He is currently a Research Engineer with Scientific Systems Company, Inc., Woburn, MA. His research interests include distributed control and estimation, optimization and control of networked dynamical systems, and motion coordination and vision-based control of unmanned air and ground vehicles.



Nathan Michael (S'05–M'09) received the Ph.D. degree in mechanical engineering from the University of Pennsylvania, Philadelphia, in 2008.

He is currently a Research Scientist at the GRASP Laboratory, University of Pennsylvania. His current research interests include control and estimation for multirobot systems and experimental robotics.



Ali Jadbabaie (S'99–A'02–M'03–SM'07) received the B.S. degree (with high honors) from Sharif University of Technology, Tehran, Iran, in 1995, the Master's degree in electrical and computer engineering from the University of New Mexico, Albuquerque, in 1997, and the Ph.D. degree in control and dynamical systems from California Institute of Technology, Pasadena, in 2001.

From July 2001 to July 2002, he was a Postdoctoral Associate with the Department of Electrical Engineering, Yale University, New Haven, CT. In July 2002, he joined the University of Pennsylvania, Philadelphia, where he is currently an Associate Professor with the Department of Electrical and Systems Engineering, and the General Robotics, Automation, Sensing, and Perception Laboratory. His research interests include network science and cooperative and distributed control of multiagent systems.

Dr. Jadbabaie is a recipient of a National Science Foundation Career Award, an Office of Naval Research Young Investigator Award, a Best Student Paper Award (as an advisor) at the American Control Conference, the George S. Axelby Outstanding Paper Award from the IEEE Control Systems Society, and the O. Hugo Schuck Best Paper Award from the American Automatic Control Council.



Kostas Daniilidis (S'90–M'92–SM'04) received the undergraduate degree in electrical engineering from the National Technical University of Athens, Athens, Greece, in 1986 and the Ph.D. degree in computer science from the University of Karlsruhe, Karlsruhe, Germany, in 1992.

From 1998 to 2003, he was an Assistant Professor with the University of Pennsylvania, Philadelphia, where he is currently an Associate Professor of computer and information science as well as the Director of the interdisciplinary General Robotics, Automation, Sensing, and Perception Laboratory. His research interests include the robot perception of space, motion, and objects, with applications to location recognition, video retrieval, navigation, visual formation control, omnidirectional vision, and immersive environments.

Dr. Daniilidis is an Associate Editor of the IEEE TRANSACTIONS ON PATTERN ANALYSIS AND MACHINE INTELLIGENCE and the founder of the IEEE Workshop Series on Omnidirectional Vision and Camera Networks. He was the Area Chair of the 2004 European Conference on Computer Vision, the IEEE Conference on Computer Vision and Pattern Recognition in 2004, 2005, and 2006, and the 2007 International Conference on Computer Vision. He was also the Co-Chair of the Third Symposium on 3-D Data Processing, Visualization, and Transmission.